The Particle-Forming Process of SiO_2-Supported Metallocene Catalysts

Gerhard Fink*, Bernd Tesche, Frank Korber, Stefan Knoke

Max-Planck-Institut für Kohlenforschung, Kaiser-Wilhelm-Platz 1,

45478 Mülheim an der Ruhr, Germany

SUMMARY: Homogeneous metallocene catalysts for the polyolefin production show compared with conventional Ziegler systems remarkable advantages, like the possibilities to regulate the microstructure leading to optimized polymer properties. However, for industrial application it is necessary to immobilize the metallocenes on a heterogeneous support. The parameters which now influence polymerization kinetics, polymer growth, polymer morphology, the decisive particle fragmentation are demonstrated and summarized in a physical and mathematical model.

Introduction

A growing global demand for polyolefins and their copolymers as well as the necessity to optimize their quality have led to an intensive research in the field of supported metallocene catalysts.[1)] Well-defined microstructures, high activity, narrow molar mass distributions and the possibility of tailor-made polymers are the main advantages of metallocene catalysts in comparison to classical Ziegler or Phillips catalysts.[2)]

By heterogenization an easy application of these metallocenes within existing slurry and gas-phase processes and reactors is possible ("drop-in catalysts"). Furthermore, heterogenization leads to other advantages such as high bulk density, little reactor fouling and good morphology. Figure 1 visualizes some of the most important parameters that affect the polymer properties.

For example the catalyst carrier (silica gel in normal case) has to be relatively stable to avoid polymer fines but on the other hand it has to permit the subsequent fragmentation of the catalyst into sub-micrometer range primary SiO_2-particles induced by the hydraulic forces of the growing polymer. These very small particles do not disturb the further procession.[3)]

The size of these initial primary particles is determined during the design and the preparation of the support. In addition to that the supporting procedure is decisive for the distribution degree of the catalytic components metallocene and methylalumoxane (MAO) on and in the particle. Presently only by suspension impregnation a homogeneous distribution over the whole particle is achieved. Gas-phase impregnation leads to inhomogeneous distributions, because metallocene/MAO components are not able to penetrate the inner particle.

 CCC 1022-1360/00/$ 17.50+.50/0

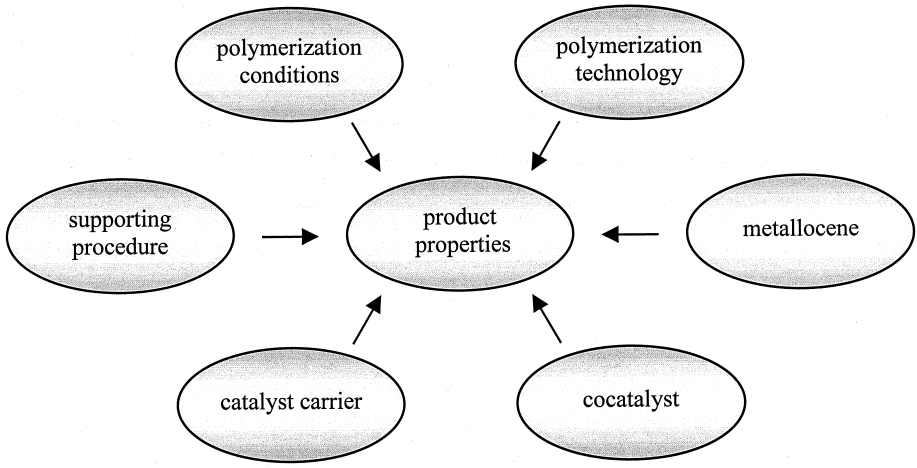

Fig. 1: Parameters which influence the polymer structure and polymer properties

Two further important points of figure 1 are the polymerization conditions and the polymer reaction engineering. The reaction engineering deals with the kind of process which may be gas phase, bulk and slurry process. In combination with a specific choice of the polymerization conditions we chose the slurry polymerization process for our extensive kinetic studies. Together with low temperatures, low monomer and catalyst concentrations we were able to slow down the polymerization process. This allows us to examine the "single sections" (figure 2) of the process carefully. Thus the variety of parameters, necessary to control the polymerization process, build a complex network of mutual relations and interactions. It is a purpose of our research to investigate such parameters and to understand their interrelating effects. Therefore we are able to comprehend the polymerization process as a whole and consequently we are capable of optimizing the process with regard to the polymer properties.

Fragmentation Model for Propene Polymerization with Silica-supported Metallocenes

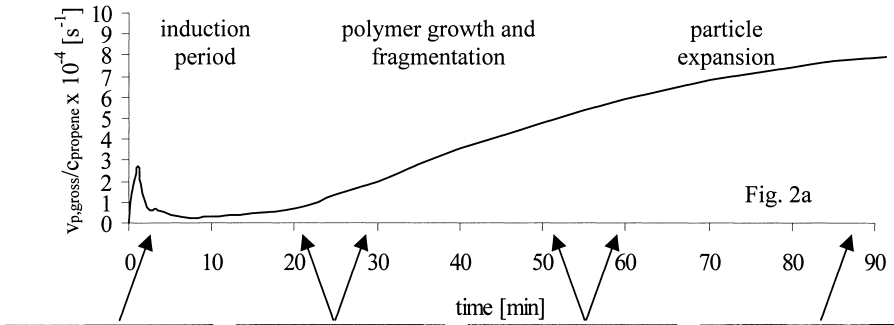

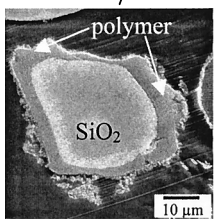

Fig. 2b

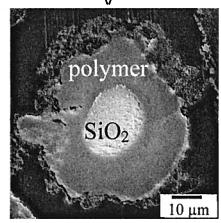

Fig. 2c

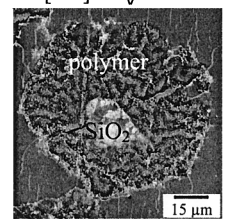

Fig. 2d

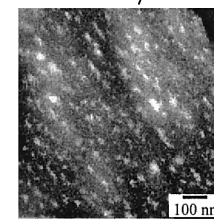

Fig. 2e

Fig. 2: Stages of particle growth in slurry polymerization:
Fig. 2a shows the typical kinetic profile of a slurry polymerization with a silica supported metallocene catalyst. Fig. 2b-d show scanning electron microscopy (SEM) images of catalyst grains, embedded in epoxy resin and sectioned. Fig. 2e shows a transmission electron microscopy (TEM) image in negative contrast of an ultra thin section of an embedded catalyst grain. All electron microscopy images are assigned by arrows to corresponding polymerization stages in figure 2a.

The graph of figure 2 shows the polymerization rate normalized on the propene concentration as a function of the polymerization time. The polymerization process can be divided into four different sections. First the polymerization rate shows an initial maximum which results in a coating of the catalyst particle surface with polymer. After this, a period of low activity occurs (induction period) as the coating limits the diffusion of the monomer. When enough monomer molecules have reached the inner polymerization active centers by diffusion through the polymer coating the third section starts. The polymerization rate rises and we have polymer growth with silica carrier fragmentation. Finally, a broad maximum of activity is reached and particle expansion starts. We want to give you a more detailed description in the following:

The polymerization starts at the active centers on the surface of the particle, because access to them is without hindrance. On the outer surface of the silica support and to some degree below the surface (subcutaneous) the thin polymer boundary layer is formed during this initial stage. This thin cover consists of highly crystalline polypropene with up to 75 % crystallinity. Corresponding to this in figure 2b the lighter region represents silica, the darker region polymer. This polymer layer works as a diffusion barrier for the monomer supply, so that the diffusion of propene molecules through this layer becomes the rate determining step of the polymerization reaction. As a consequence, the high initial polymerization activity decreases sharply during the first minutes and a period of relative low polymerization activity (figure 2a) is reached. The length of this period can vary notably and is a function of some parameters like temperature, monomer concentration and particle diameter. Polymer is growing from the outer shell towards the center of the carrier and gradually breaks down the carrier more and more. A continuous increase in polymerization activity is observable in the kinetic profile (figure 2a). As a consequence of the increasing activity the silica support gets fragmented by the hydraulic forces of the growing polymer. This process continues towards the center until the whole support is fragmented and all active sites are accessible for monomer molecules. In figure 2d only a small core of unfragmented silica coated by a thick layer of polymer with silica fragments is left. An interesting detail in figure 2d is the wavy surface of the polymer phase. This is a preparation artifact from the sectioning process, due to differences in the degree of hardness of embedding resin, polymer and bulk silica. This demonstrates that we have now a polymer matrix with fragmentized silica particles. Finally, in figure 2e the silica support is completely fragmentized into particles in the size range of about 50 nm and below. They are homogeneously distributed in the polymer matrix. Now, the maximum polymerization activity is achieved and a significant particle expansion starts and lasts much longer as shown in figure 2a.

By means of this polymer growth and particle expansion model we were able to design a mathematical simulation of the whole polymerization process. For this mathematical simulation we developed a “shell by shell”-fragmentation approach – a gradual disintegration of the shell from the outside to the inside. This has enabled us to determine the rate constants for the activation, propagation, mass and heat transfer and termination steps of the polymerization process. Further we succeeded to transfer it to the mathematical simulation of the polymerization kinetics affiliated with grain diameters of different size.[4) - 6)]

Looking back to figure 2b - e we now discuss the phenomenon of the particle expansion in some more detail.

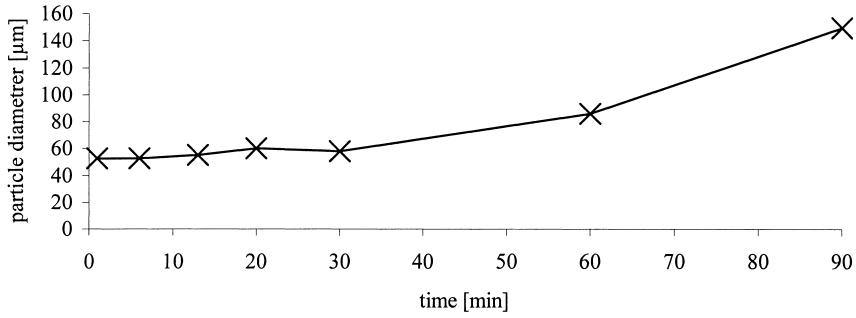

Fig. 3: Mean particle diameter as a function of polymerization time, measured from SEM micrographs.

Figure 3 demonstrates one example of the dependence of the particle diameter on the polymerization time. During the first 30 minutes here the particle size remains nearly constant. The reason for this is the coating around the particle surface described above. In the course of the next 30 minutes the particle diameter starts to grow moderately. This slight polymer growth is accompanied by the beginning fragmentation of the silica support.

After about 90 minutes a threefold increase of the initial particle diameter can be observed here. This is connected with the particle expansion phase of our model. Thus, the observations support our model in a comprehensive way. The further expansion process of the particle up to the mm scale is theme of figure 5, which is received from bulk polymerization experiments. The results of all our experiments indicate that despite the large differences of experimental conditions between the slurry and the bulk process { slurry process: [Zr] = 1 x 10^{-4} mol/L; p(propylene) = 2 bar; [Zr] : [TIBA] = 1 : 200; T_P = 40°C; V(reactor) = 0.25 L; V(toluene) = 0.1 L; bulk process: [Zr] = 1 x 10^{-6} mol/L; T_P = 50°C; p(propylene) corresponds to the respective vapour pressure and is around 21 bar; [Zr] : [TIBA] = 1 : 2000; V(reactor) = 1.8 L; m(propylene) = 457 g }, our polymer growth and particle expansion model not only applies to the slurry process but also to the bulk process. This is an essential benefit of our model, because it enables a comprehensive and complete description of the polymerization process.

Another important thing is the course of the crystallinity of polymer in dependence of the polymerization time.

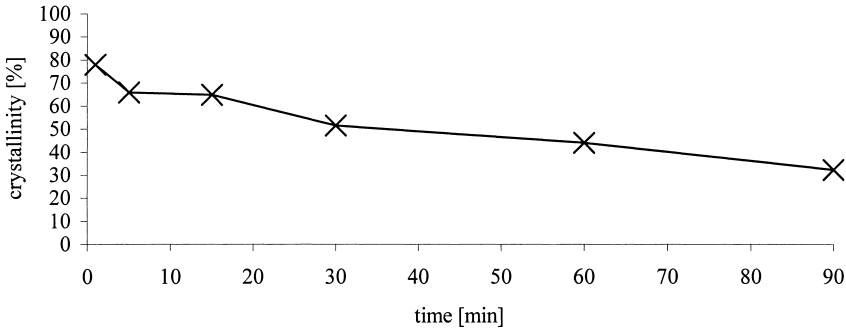

Fig. 4: Crystallinity of polypropene resulting from DSC-measurements as a function of the polymerization time.

According to figure 4 after definite times polymerization was terminated and the resulting polymer samples have been DSC-measured and crystallinity was calculated.

The high crystallinity in the beginning represents the polymer from the initial polymer coating. Then crystallinity decreases significantly during the proceeding polymerization process (particle fragmentation, particle expansion). Furthermore, microstructure-analysis via NMR shows an increase of stereo- and especially of regio-errors in the same dependence of the polymerization time. We think these phenomena are correlated with changes in heat transfer. At the beginning we find the highest crystallinity, because heat transfer from the particle in the bulk is not influenced. Afterwards, the heat transfer in the inside of the definite particles deteriorates. So a heat increase in the discrete particles occurs and causes the growing number of regio-errors.

Polypropene Growth During Bulk Phase Polymerization

Now we return to the further expansion of the polymer particle as discussed in figure 3. One of our current aims is to investigate and understand the industrially relevant mass polymerization process carried out in liquid monomer.[7)] As in this process it is not possible to measure kinetics in the established way using flow meter technique, we introduced reaction calorimetry as an innovative tool for our kinetic studies. With calorimetric techniques it is possible to measure the heat released during a polymerization. According to the following equation this heat (Q_r) is proportional to the polymerization rate (v_P), our response value:

$$Q_r = v_P * (-\Delta H_P)$$

(Q_r: heat generation rate of chemical reaction [W]; v_P: rate of polymerization [mol/s]; $(-\Delta H_P)$: heat of polymerization of the monomer [J/mol]).

Using a modified $RC1_e$ heat flow calorimeter of the Mettler Toledo AG we are now able to study the bulk polymerization process in some detail. Doing this we will have to address problems arising from the increase in viscosity during the reaction and the accompanying difficulty in removing the heat involved.

Figure 5 shows a typical kinetic profile of a propene mass polymerization at T = 50°C in combination with the regarded particle growth. According to the polymer growth and particle expansion model arising from our experiments in toluene slurry phase it is obvious that even under these technically relevant conditions diffusion limitations during the reaction are of major importance. In analogy to figure 2a we find a kind of prepolymerization period in the first minutes of the polymerization, which is almost directly followed by a comparable increase of activity caused by the fragmentation process. Finally, this increase leads to a broad maximum of activity.

Spherical particles with a good morphology and particle diameters of up to 4 mm are formed which meet industrial process demands.

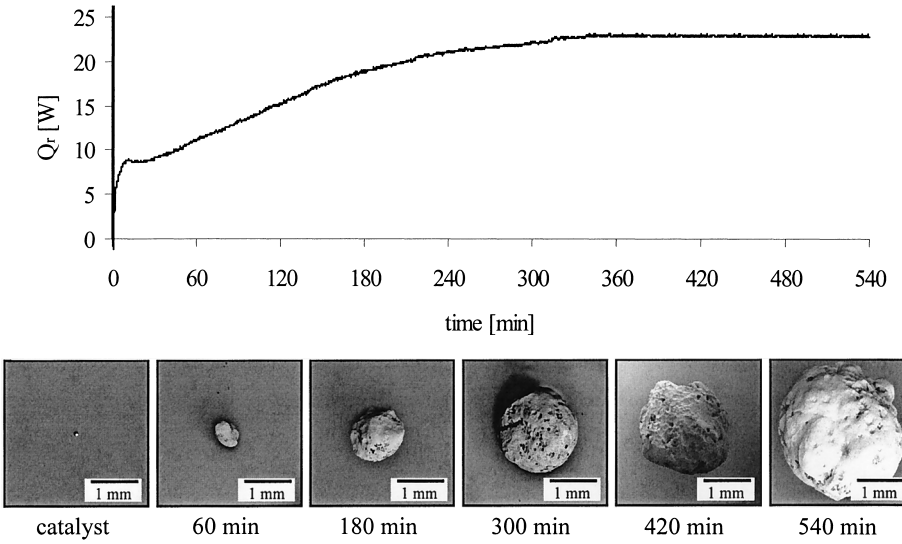

Fig. 5: Heat generation of a propene mass polymerization as a function of the polymerization time and visualization of the particle growth

3D-Reconstruction of a Porous Catalyst Particle

To arrive at the excellent morphology characteristics of polyolefins made by the latest generation of heterogeneous Ziegler-Natta catalysts, metallocenes are impregnated on suitable inorganic supports. Of all tested materials, silica proved to be the best because of its high specific surface and porous structure. In order to achieve a better understanding of the heterogeneous polymerization process and the influence of the support structure during polymer growth, it is necessary to determine the inhomogeneity of both the external surface and the internal pore structure. We were able to generate a 3D-reconstruction of a support particle by means of electron micrographs taken from serial sections of the embedded materials.

The 3D-reconstruction of a porous particle utilizes an image processing routine that requires the development of a suitable sample preparation technique: silica supports (with particle diameters varying between 40 μm and 60 μm) were embedded in a commercial Spurr-resin and cut into thin sections with an ultramicrotome. Figure 7 shows an SEM-micrograph of a resin block with embedded silica particles (silica white, cavities filled with resin black). 240 serial sections (thickness about 70 nm) were mounted on gold-coated glass supports. SEM-images of each section generate digital images of the particle of interest which were transformed into a binary data set for the digital image processing.

The results are summarized in figure 8 and 9: Figure 8 shows the processed micrographs of a selected particle after 36 serial sections. The arithmetical addition of the gray values allows conclusions to be reached regarding the morphology of the cavities within the respective sector. Figure 9a demonstrates the digital reconstruction of two-thirds of one particle, starting with the first section. The entire 3D-reconstruction enables us to look at the particle from different projections and to focus on special bulk cavities through the particle (figure 9b, 9c). The digitally available tomographical particle reconstruction enables us, for example, to follow a single micro pore on its way through the support particle and get an impression of the pore structure in dependence on the external surface.

This 3D-reconstruction of a porous particle has to be regarded as a first step admittedly. We want to point out that an active catalyst based on the investigated support particles might look different due to substantial MAO loading. But we were already able to perform 3D-reconstructions of prepolymerized catalyst particles. Results referring to this are already documented[8)] and will be published soon in a separate paper.

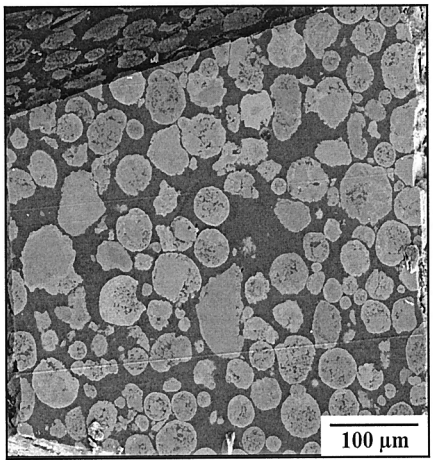

Fig. 7: SEM-micrograph of sectioned SiO_2-supports embedded in a resin block

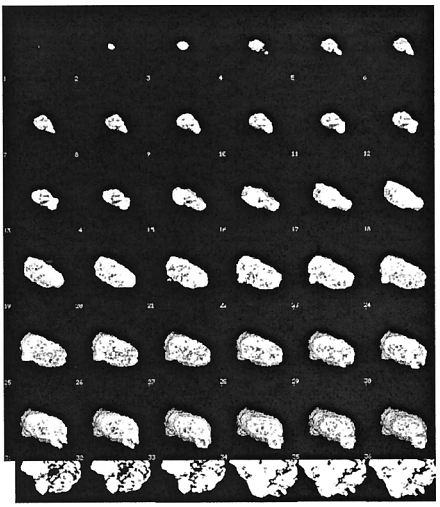

Fig. 8: Projection of 36 serial sections

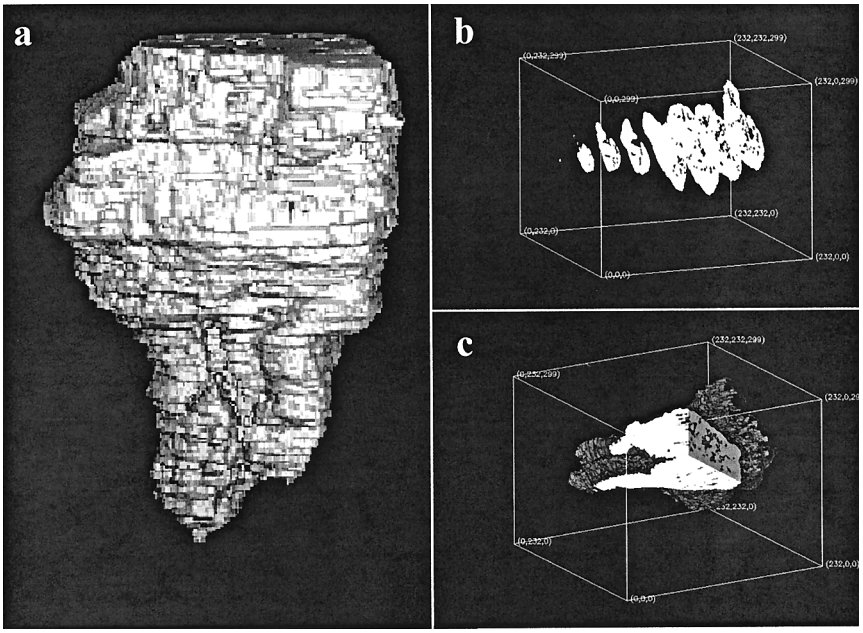

Fig. 9: Different projections of an SiO_2-particle, reconstructed from 240 serial sections

Outlook

As a result of our detailed kinetic and electron microscopic studies of the propene slurry process we were able to develop a polymer growth and particle expansion model which describes the total polymerization process. Concerning the liquid propene polymerization we are on the way to such a model for the complete process whereby we will have to address problems arising to the increasing viscosity during the reaction and the accompanying difficulty in removing the head involved. Finally, in order to be able to obtain insitu kinetic information from the gas phase polymerization process, we are currently introducing video microscopy in combination with digital image processing techniques as a new tool to our analytical equipment. We will evaluate individual particle kinetics as well as statistical relevant polymer growth kinetics in gas phase propene polymerization.

References

1. C. Jenny, P. Maddox, *Curr. Opin. Solid State Mater. Sci.* **3,** 94 (1998)
2. B. Steinmetz, J. Zechlin, C. Przybyla, B. Tesche, G. Fink, *Nachr. Chem.* **48**, 12 (2000)
3. G. Fink, B. Steinmetz, J. Zechlin, C. Przybyla, B. Tesche, *Chem. Rev.* **100**, 1377 (2000)
4. C. Przybyla, J. Zechlin, B. Steimetz, B. Tesche, G. Fink, in: *Metalorganic Catalysts for Synthesis and Polymerisation,* W. Kaminsky (Ed.), Springer, Berlin 1999, p. 321-332
5. C. Przybyla, J. Zechlin, B. Steimetz, B. Tesche, G. Fink, in: *Metalorganic Catalysts for Synthesis and Polymerisation,* W. Kaminsky (Ed.), Springer, Berlin 1999, p. 333-346
6. J. Zechlin, B. Steinmetz, B. Tesche, G. Fink, *Macromol. Chem. Phys.* **201**, 515-524 (2000)
7. J. Zechlin, K. Hauschild, G. Fink, *Macromol. Chem. Phys.* **201**, 597-603 (2000)
8. B. Steinmetz, Dissertation, Heinrich-Heine-Universität Düsseldorf, 2000